 doi:10.20944/preprints202111.0119.v1

Review

Carbon-Based Materials in Photodynamic and Photothermal Therapies applied to Tumor Destruction

Karina Janeri Lagos[1], Hilde Harb Buzza[2,3], Vanderlei Salvador Bagnato[2], María Paulina Romero [1,*]

[1] Department of Materials, Escuela Politécnica Nacional (EPN), 170525, Quito, Ecuador; karina.lagos@epn.edu.ec (K.J.L.)
[2] São Carlos Institute of Physics, University of São Paulo (USP), 13566-590, São Carlos, Brazil; vander@usp.br (V.S.B.)
[3] Institute of Physics, Pontificia Universidad Católica de Chile, 7820436, Santiago, Chile. hilde.buzza@fis.uc.cl

* Correspondence: maria.romerom@epn.edu.ec (M.P.R.)

Abstract: Within phototherapy, a grand challenge in clinical cancer treatments is to develop a simple, cost-effective, and biocompatible approach to treat this disease using ultra-low doses of light. Carbon-based materials (CBM), such as graphene oxide (GO), reduced GO (r-GO), graphene quantum dots (GQDs), and carbon dots (C-DOTs), are rapidly emerging as a new class of therapeutic materials against cancer. This mini-review summarizes the progress in lasts years regarding the applications of CBM in photodynamic (PDT) and photothermal (PTT) therapies for tumor destruction. The current understanding of the performance of modified CBM, hybrids and composites, is also addressed. This approach seeks to achieve an enhanced healing action by improving and modulating the properties of CBM to treat various types of cancer. Metal oxides, organic molecules, biopolymers, therapeutic drugs, among others, have been combined with CBM to treat cancer by PDT, PTT, or synergistic therapies.

Keywords: phototherapy; cancer; graphene oxide; reduced graphene oxide; graphene quantum dots; carbon dots.

1. Introduction

Phototherapy is a new non-traditional strategy that has been used within several bio-applications. For example, in antimicrobial treatments, light stimulation of an agent promotes the inactivation of bacteria, protozoa, viruses, and fungi [1–3]. Likewise, various diseases such as vitiligo [4], psoriasis [5], atopic dermatitis [6], cancer [7], and so on have been diagnosed and treated by this approach.

Cancer has become a disease of significant concern in recent years due to its threat to human life, causing millions of deaths [8]. Thus, several studies have proposed phototherapy, using nanomaterials as photoabsorbing agents, as an alternative to treat cancer [9–11]. It is worth noticing that phototherapy is advantageous compared to radiotherapy, chemotherapy, or surgery owing to their simple operation, minimally invasive procedure, reduced toxicity, minor trauma, fewer adverse reactions, and negligible drug resistance [12,13]. Nevertheless, it has drawbacks as poor penetration, which limits its action in deep tumors. Photodynamic therapy (PDT) and Photothermal Therapy (PTT) are encompassed within phototherapy. When a suitable wavelength of light is irradiated upon a defined molecule photosensitizer (PS) or photothermal agent (PA), reactive oxygen species (ROS) and heat are generated, respectively, in PDT and PTT. In both cases, these responses are used to damage malignant cells in cancer [14,15]. In PDT, the PS is excited by light; in this state, the PS reacts with nearby molecular oxygen and generates ROS, either type I (free radicals) or type II (singlet oxygen, $^1O_2$) reactions. In cancer treatments, this action results in apoptosis, necrosis, or autophagy of the abnormal cells inhibiting the tumor growth [16]. The efficiency of PDT is related to the

ROS generation yield, which depends on the PS, dose, source light, and tissue oxygen [17]. About PTT, it is based on localized hyperthermia. The PAs are irradiated by light and they absorb photons, which produces an excited state. By non-radiative relaxation pathways, heat is generated to dissipate this excess of energy [18]. When the temperature of the PAs surrounding the environment rises, malignant cells are destroyed due to their low heat tolerance than normal cells. Thus, the targeting capability of photothermal agents in tumor cells is one of the keys [19,20].

In both therapies, PDT and PTT, particular properties in their active agents are required, robust responses to light stimuli. Furthermore, high specificity, biocompatibility, low dark toxicity, and optical characteristics are desirable [21]. On this basis, carbon-based materials (CBM) have become excellent candidates as phototherapy agents and platforms or carriers of these compounds [22–25]. The specificity of CBM accomplishes to focus its action only on damaged cells. These materials are critical components due to their remarkable advantages, such as reduced side effects and low toxicity in specific concentrations [16,26]. Phototherapy agents can also be loaded with drugs or combined with other materials to enhance their healing action or to improve and modulate their properties, making possible the coalesce of distinct mechanisms of action [27]. Thus, the doping and hybrids fabrication of CBM along synergistic therapies are also addressed in this mini-review.

2. Carbon-based materials (CBM) applied in photodynamic (PDT) and photothermal (PTT) therapies

CBM has been considered phototherapy agents due to its remarkable features. Nevertheless, it is worth noting that the properties of any CBM vary according to its specific structure (size and shape), which is determined by the method of synthesis, along with its experimental conditions and carbon source nature. About the latter, some authors have even proposed using residues such as bio-mass and polymers waste for this aim [28,29]. To synthesize CBM, two approaches have been employed (i) top-down, reduction of size from bulk materials, such as mechanical or chemical exfoliation, and (ii) bottom-up, construction from the atomic level, like epitaxial growth and chemical vapor deposition [30,31].

Within CBM, graphene has become one of the most studied materials owing to its unique chemical and physical properties [32,33], which have encouraged its application in diverse fields such as electronics, material science, energy, and biomedicine, including the treatment of COVID-19 disease [34–37]. Regarding bio-applications, the versatility of graphene has allowed its assessment as an antimicrobial agent [38], in sensors [39], in drug delivery [40], bioimaging [41], regenerative medicine [42], cancer treatment [43,44], and photodynamic and photothermal therapies [45,46]. However, the hydrophobicity of the pristine graphene has turned into a drawback when affinity with physiological solutions or water is desirable [47]. Besides, graphene tends to agglomerate in solution and has poor solubility. In this context, some alternatives have been proposed to overcome this limitation. For example, functionalized graphene derivatives such as graphene oxide (GO), reduced graphene oxide (r-GO), or graphene quantum dots (GQDs) have been employed instead. These derivatives have excelled as novel materials due to their large specific surface area, bio-compatibility, solubility, and selectivity [48,49]. Another enthralling new material with comparable properties to those of graphene derivatives is carbon dots (C-DOTs). These 0D materials with sizes below 10 nm and easy to synthesize have also been extensively used in bio-applications [50–52].

In this section, GO, r-GO, GQDs, C-DOTs, and their composites and hybrids are addressed as new materials in phototherapy and synergistic therapies against cancer disease.

2.1 Graphene oxide (GO)

Preprints (www.preprints.org) | NOT PEER-REVIEWED | Posted: 5 November 2021 doi:10.20944/preprints202111.0119.v1

GO has a 2-dimensional (2D) honeycomb structure, with sp3 domains enclosing sp2 carbon domains, is covalently functionalized with carbon and oxygen groups [53]. These attachments are which differentiate GO from graphene. The presence of carboxylic (-COOH), hydroxyl (-OH), carbonyl (C=O), alkoxy (C-O-C), epoxy (>O), or other functional groups induce changes in specific GO properties such its characteristic insulator behavior and water affinity [54,55]. The functionalization allows establishing covalent bonds with other species. Few studies have reported sulfur contents in GO, which also induce substantial variations in its acidic and electric properties [56]. Worth indicating that these couplings trigger an expansion in the interlayer spacing, doubling the GO size compared to graphene. Generally speaking, the properties of GO consist of the planar layer structure, high thermal and electrical conductivity, excellent optical transmittance, and flexibility of surface modification [57].

A simplified scheme of GO applications (advanced delivery system, phototherapy, and bioimaging) is presented in Figure 1.

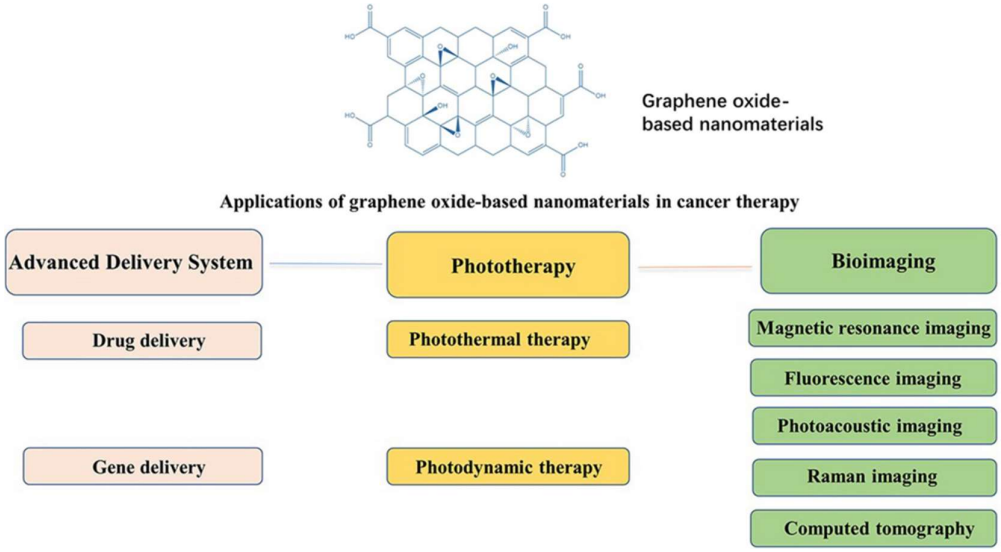

Figure 1. Applications of graphene oxide-based nanomaterials in cancer therapy. Reproduced from Ref. [58] with permission from Springer Nature.

2.1.1 Application of GO in PDT

Based on PDT, several studies have shown GO and standard photosensitizers (PS) for cancer treatment. Hosseinzadeh R. (2018) fabricated a PS using GO and methylene blue. The killing cancer cell potential of the PS was evaluated by Thiazolyl Blue (MTT) cell viability assay, employing a human breast cancer cell line (MDA-MB-231). The results showed a reduction of up to 20% of cell viability, using a concentration of 20 μg/mL and under red LED illumination (630 nm), being a much better performance than the components separately or in dark conditions [59]. Likewise, Sun X. et al. (2018) developed a GO-based nanocomposite. For this, they encapsulated TPE-red (tetraphenylethylene-aggregation-induced emission nanoparticles) with modified GO by PEGylation procedure. They demonstrated that the nanocomposite increased the production of ROS under laser irradiation of 450 nm, enhancing the ROS generation capability compared to single TPE-red. Besides, an MTT assay was carried out on UMUC3 cells indicating higher toxicity under radiation than in dark conditions. [60]. Qin et al. (2018) fabricated a nanocomposite with GO, magnetic nanoparticles (Fe_3O_4), chitosan and a novel photosensitizer HNPa (3-[1-hydroxyethyl]-3-divinyl-131-b,b-dicyano-methylene-131-deoxopyropheophorbide-a). They confirmed a superior singlet oxygen quantum yield compared to the single HNPa, being 62.9% and 42.6%, respectively. Also, they demonstrated that the presence of GO-Fe_3O_4 accelerated the penetration of HNPa into the

Preprints (www.preprints.org) | NOT PEER-REVIEWED | Posted: 5 November 2021 doi:10.20944/preprints202111.0119.v1

nucleus of the human hepatocellular carcinoma cell line (HepG-2). Besides, an MTT assay carried out under 698 nm of irradiation verified an enhanced result of HNPa to increase photodynamic cancer cell death [61].

A simplified scheme of GO-composite application in PDT is shown in Figure 2.

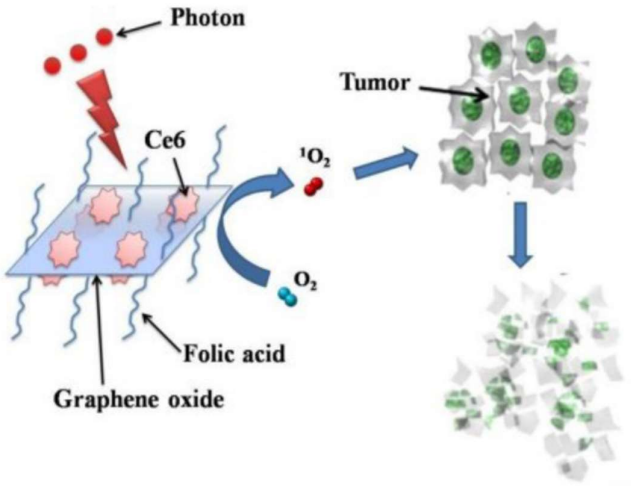

Figure 2. PS molecules of Chlorin e6 (Ce6) loaded by folic acid–conjugated GO for PDT applications in cells. Reproduced from Ref. [62] with permission from PubMed Central.

2.1.2 Application of GO in PTT

The excellent efficiency of GO photothermal conversion in the NIR region makes it susceptible to use in PTT [63]. In recent years, highly elaborate hybrids have been developed to improve the solubility and selectivity of GO for this aim. Lim et al. (2018) fabricated a ~155 nm nanocomposite using GO along folic acid and manganese dioxide (MnO_2). In cancer, the MnO_2 decomposes hydrogen peroxide into oxygen, relieving hypoxia. The results showed that the composite heat capacity was better than a single GO. Under 808 nm laser excitation of 3.5 min, the nanocomposite reaches the desired temperature of 47°C while GO reaches barely 35°C [64].

Similarly, Xie et al. (2019) fabricated a composite with good stability and dispersibility from: GO, magnetic nanoparticles (Fe_3O_4), chitosan, sodium alginate, and doxorubicin hydrochloride (DOX). They verified the composite PTT properties using an MTT assay with human lung cancer cell line (A549) and irradiation of 808 nm for 5 min, demonstrating excellent intracellular uptake characteristic and dependence of the increase in temperature with the concentration. The best result showed a reduction of the survival rate to 14.36% with a dose of 100μg/mL [65]. Also, in the study of Huang and coworkers (2019), they developed a composite with indocyanine green (IR820), lactobionic acid, DOX, and GO. They compare the photothermal capabilities of the composite and single GO, verifying a better performance of the composite due to an increase in temperature of 16.6 °C and 8.2 °C, respectively, after 5 min of irradiation of 660 nm [66].

2.1.3 Application of GO in synergistic therapy

A synergistic effect results from two or more processes interacting together to produce an effect that is greater than an individual effect. The assembly of composites through different materials with complementary properties allows its application in synergistic therapy [67]. Several authors have studied the PDT / PTT synergistic effect of GO-based nanocomposites. Gulzar et al. (2018) fabricated a hybrid with GO, amino-modified upconversion nanoparticles ($NaGdF_4:Yb^{3+}/Er^{3+}@NaGdF_4:Nd^{3+}/Yb^{3+}$), polyethylene glycol, and Chlorin e6 (Ce6). Singlet oxygen generation was confirmed through the DPBF (1,3-diphenyliso- benzofuran) chemical probe (PDT effect). In addition, in vivo antitumor

Preprints (www.preprints.org) | NOT PEER-REVIEWED | Posted: 5 November 2021 doi:10.20944/preprints202111.0119.v1

property was evaluated in mice using a U14 (murine hepatocarcinoma) cell line with irradiation of 808 nm. As a result, a significant tumor size decrease was achieved owing to the PTT effect [68]. Zhang et al. (2019) tested PDT, PTT, and chemotherapeutic effects of a composite fabricated with GO, wedelolactone, and indocyanine green. Under NIR irradiation (808 nm), ROS (singlet oxygen) generation was confirmed by DCFH-DA probe in HeLa cells (human cervical carcinoma cells). Besides, stable and high heat reaching were proved (~79°C) in comparison to the individual components (~33°C) [69]. Romero et al. (2021) functionalized GO surface modified with PEG-folic acid, rhodamine B, and indocyanine green to treat Ehrlich tumors in mice by in vivo experiments using PDT and PTT with a NIR light of 808 nm 1.8 W/cm^2. Based on fluorescence images of the tumor, the highest concentration of GO as a function of the time after intraperitoneal injection was determined [70].

A basic scheme of the procedure to apply GO in synergistic therapy is shown in Figure 3.

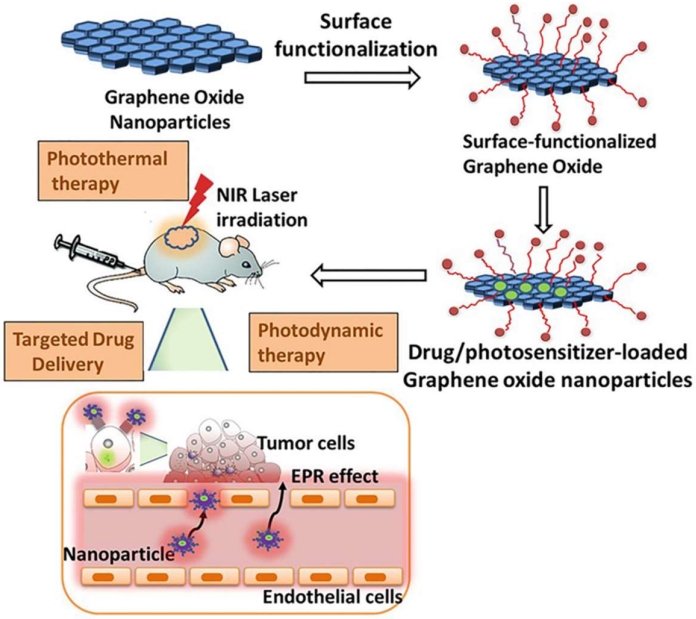

Figure 3. Procedure to apply GO-based hybrids/composites in PDT, PTT, and targeted drug delivery. EPR: enhanced permeability and retention. Reproduced from Ref. [57] with permission from MDPI.

2.2. Reduced graphene oxide (r-GO)

r-GO is a material that exhibits excellent graphene-like properties. Generally, it is obtained from GO by some methods. Thermal, chemical, photocatalytic, laser, and electrochemical treatments, among others, have been developed to carry out the reduction from GO to r-GO [71]. In these procedures, functional groups are removed from the GO surface, and a structure similar to graphene is achieved but with some imperfections and different magnitudes. The C/O ratio is the primary indicator to verify the quality of the GO reduction [55,72].

Several applications such as catalysts, membranes, super-capacitors, flexible sensors, bio-applications, and more are based on r-GO [73]. Regarding the latter, specifically in phototherapy, r-GO is considered an excellent PS due to its ability to absorb visible and near-infrared ranges over the whole spectrum. Within cancer disease treatment, r-GO can be functionalized using conjugated molecules, which can be employed as a drug delivery platform. Thus, r-GO has been employed in some therapies against cancer, as shown in Figure 4.

Preprints (www.preprints.org) | NOT PEER-REVIEWED | Posted: 5 November 2021 doi:10.20944/preprints202111.0119.v1

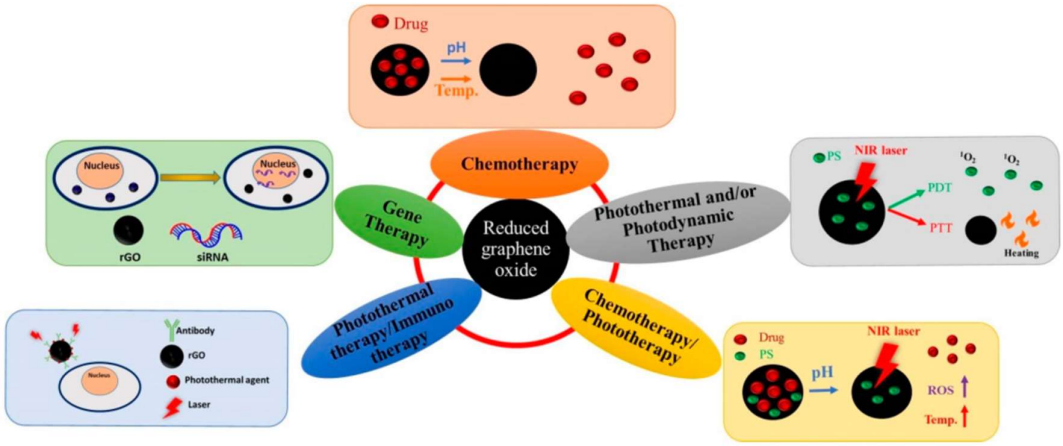

Figure 4. Applications of r-GO in PDT and PTT Therapy, chemotherapy/phototherapy, photothermal/immune therapy, and gene therapy. Reproduced from Ref. [74] with permission from MDPI.

2.2.1 Application of r-GO in PDT

Highly elaborated hybrids have been developed in recent years to improve the r-GO solubility and selectivity in PDT applications. Thus, Kapri and Bhattacharyya (2019) synthesized a composite with nitrogen-doped r-GO, molybdenum sulfide, manganese dioxide, and PEG to test its photodynamic properties against cancer. They employed the MTT assay with HeLa cells and HEK 293 cells (human embryonic kidney cells), demonstrating excellent cell killing efficiency for both cases. They used NIR irradiation of 980 nm, achieving a disproportionation production of intracellular H_2O_2 turning this composite to an enhanced PS [75]. Likewise, Vinothini and coworkers (2020) developed an rGO-based composite with magnetic nanoparticles (Fe_3O_4), camptothecin, 4-hydroxycoumarin, and allylamine, to evaluate its photodynamic capability. They demonstrated high ROS generation and consequently good inhibition against human breast cancer cell lines (MCF-7) under 365 nm of laser irradiation [76]. Green approaches have also been proposed for this aim. Jafarirad et al. (2018) fabricated three hybrids with r-GO, zinc oxide (ZnO), neodymium (Nd), and silver (Au) nanoparticles (ZnO/r-GO, Nd-ZnO/r-GO, and Ag-ZnO/r-GO) using a rosehip extract (Rosa canina L.) as stabilizing and reducing agent. They satisfactorily demonstrated its antitumor capability employing 630 and 810 nm wavelengths of irradiation [77].

2.2.2 Application of r-GO in PTT

r-GO has a good photothermal conversion effect and can effectively produce an overheating effect when used with IR light. Lima-Souza et al. (2018) developed an r-GO nanocomposite using hyaluronic acid and PMAO (poly maleic anhydride-alt-1-octadecene). The hyaluronic acid was carefully chosen due to its hydrophilic behavior and targeting capacity to CD44 receptors in the cancer cells membrane. This formulation presented heat capacity since, after NIR irradiation, its temperature increased to 33°C, which induced the cancer cells death. In addition, enhanced cytocompatibility and stability were achieved in comparison to single r-GO [78]. Likewise, different light source as low-intensity LED has been tested in PTT. De Paula et al. (2020) employed red LED (640 nm) ablation to significantly decrease the tumor mass of mice (melanoma in B16F10 lineage cells) using an rGO-based treatment. Besides, the immune response was verified by detecting the growth in CD8+ T cells [79]. Liu et al. (2019) developed an elaborate hydrogel with carboxymethyl chitosan, r-GO, aldehyde, and polyethylene glycol. They assessed its photothermal effect and DOX controllable release under 808 nm of irradiation, obtaining promising results and a noticeable improvement due to the presence of r-GO [80].

Preprints (www.preprints.org) | NOT PEER-REVIEWED | Posted: 5 November 2021 doi:10.20944/preprints202111.0119.v1

2.2.3 Application of r-GO in synergistic therapy

Concerning synergist therapies, Zaharie-Butucel et al. (2019) combined PDT, PTT, and chemotherapy using a composite of r-GO, chitosan, IR820 dye, and DOX. Its anticancer activity was satisfactorily assessed by cell proliferation assay against C26 cells (murine colon carcinoma) under NIR irradiation of 785 nm. In addition, the authors demonstrated that the composite penetrated the cytoplasm and the nucleus using scanning confocal Raman microscopy. The composite was the tracker of the living cells, owing to the underlying lattice of the r-GO [81]. Wang et al. (2020) studied photothermal action and used an r-GO/PEG-NH_2/Fe_3O_4 composite under irradiation of 805 nm to eliminate primary tumors.

Moreover, this nanomaterial encouraged antitumor immunity [82]. Zhang et al. (2017) treated A549 lung cancer cells using two different light sources of 808 nm and 450 nm to PTT and PDT, respectively. As PS, they used a composite based on r-GO along with PEG-modified Ru (II) complex. This combination resulted in better cytotoxicity and an enhanced reduction in tumor volume, which was observed from in vivo tests [83].

A scheme of the procedure to apply an r-GO composite in synergistic therapy is shown in Figure 5.

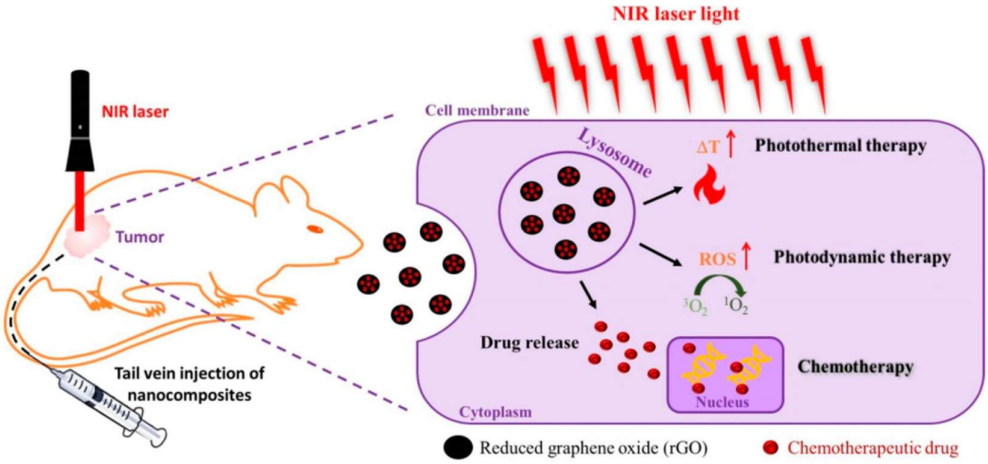

Figure 5. r-GO-based nanocomposite applied in chemotherapy, PDT, and PDT against cancer with subcutaneously implanted cancer cells in vivo. Reproduced from Ref. [74] with permission from MDPI.

2.3. Graphene quantum dots (GQDs)

The zero-dimensional GQDs are emerging graphene derivatives. Its thickness, less than 100 nm, consists of a maximum of 10 stacked layers of graphene sheets. These reduced dimensions trigger quantum confinement and special edge effects [52,84]. Due to the low toxicity, biocompatibility and photostability, GQDs have many applications such as cell imaging, drug carrier, biosensors, and so on [85].

In order to expand the narrowed visible photoluminescence of GQDs to all visible and infrared, nitrogen doping has been considered [86]. GQDs have also been employed in several phototherapy studies [87,88], including photodynamic and photothermal therapies. GQDs were used as single photo absorbing agents or in the development of composites [89].

A scheme of the applications of GQDs is shown in Figure 6.

Preprints (www.preprints.org) | NOT PEER-REVIEWED | Posted: 5 November 2021 doi:10.20944/preprints202111.0119.v1

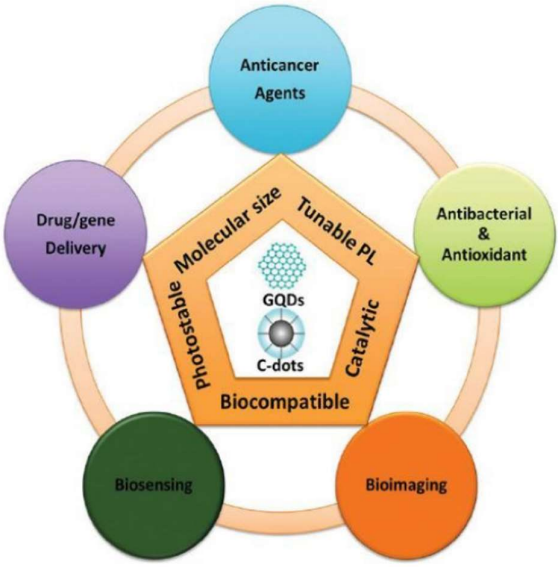

Figure 6. Applications of GQDs and carbon dots (C-DOTs) in anticancer agents, antibacterial and antioxidant, bioimaging, biosensing, and drug/gene delivery. Reproduced from Ref. [90] with permission from John Wiley and Sons.

2.3.1 Application of GQDs in PDT

Ge et al. (2014) have fabricated GQDs of 2 nm to 6 nm of diameter, which showed ROS generation capability and were employed within *in vivo* experiments. After 9 and 17 days of treatment of female BALB/c mice with GQDs, a reduction of the tumor was verified [91]. Tabish et al. (2018) synthesized 20 nm GQDs with a 7.1% yield and demonstrated its ROS generation under irradiation of 365 nm. In addition, limited toxicity was verified by *in vitro* and *in vivo* tests [92]. Campbell et al. (2021) synthesized a nanocomposite based on three covalently bounded components: nitrogen-doped GQDs, hyaluronic acid, and ferrocene. The composite was non-toxic at 1 mg/mL to HEK-293 cells but promoted cytotoxic response in HeLa cells enhanced over time. Besides, therapeutic ROS generation was three times higher than that of single ferrocene [93].

On the other hand, regarding the doping of GQDs, it has been considered to improve its phototherapy performance. Elements like sulfur and nitrogen have been employed to achieve this aim. Concerning the latter, some studies have determined that nitrogen-bonding increased ROS generation compared to single GQDs [94,95].

2.3.2 Application of GQDs in PTT

Phototherapy studies have also evaluated irradiations below the second NIR window (1000–1700 nm) to improve penetration and enhance the damage on the tumor. As a result, Liu et al. (2020) fabricated 3.6 nm GQDs and assessed their photothermal properties under 1064 nm wavelength. In vitro and in vivo tests demonstrated that GQDs killed tumor cells and inhibited tumor growth, respectively [96]. Yao et al. (2017) studied the heat generation of magnetic mesoporous silica nanoparticles capped with GQDS under an alternating magnetic field and NIR irradiation. This material showed efficient chemotherapy, PTT, and magnetic hyperthermia *in vitro* experiments [97]. Li et al. (2017) loaded IR780 dye on folic acid functionalized GQDs and studied their behavior under irradiation of 808 nm for 5 min. The temperature of a mice tumor was raised to 58.9°C, and *in vivo* antitumor experiment presented a suppressive effect on tumor growth, dissipating it in 15 days [98].

Wang et al. (2019) synthesized GQDs doped with nitrogen and boro and analyzed the composite under NIR-II region. In vitro and in vivo tests demonstrated the photothermal effect using a glioma xenograft mouse model [99].

Preprints (www.preprints.org) | NOT PEER-REVIEWED | Posted: 5 November 2021 doi:10.20944/preprints202111.0119.v1

2.3.1 Application of GQDs in synergistic therapy

Synergistic therapy has also been studied employing GQDs. Wang and coworkers (2020) developed a composite with cRGD (Cyclic Arg-Gly-Asp peptide) and DOX to evaluate its photothermal activity against SK–mel–5 and H460 cells under NIR irradiation of 808 nm. Besides, its chemotherapy capacity was verified, demonstrating an IC50 reduction up to 39.63 μg/mL and 53.75 μg/mL, respectively [100]. Likewise, Zheng et al. (2019) developed a composite with GQDs, DOX, and hollow copper sulfide nanoparticles within photothermal-chemotherapy applications using NIR irradiation on MDA-MB-231 cells. This research demonstrated a high therapeutic effect in tumor cells and its potential in cancer therapy [101]. To evaluate its NIR response, Thakur et al. (2017) produced GQDs using waste as a carbon source, specifically withered leaves of Ficus racemose (Indian fig tree). They demonstrated that GQDs were cytocompatible employing cell cycle analysis by flow cytometry and biocompatibility studies. Moreover, it was determined that upon irradiation of 808nm wavelength (0.5 W cm2), concentration dependence of photothermal response and production of reactive oxygen species [102].

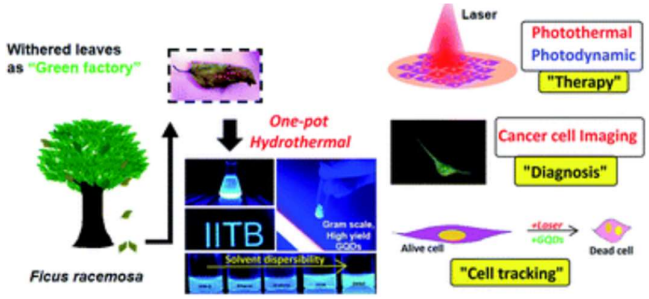

Figure 7. GQDs synthesized by hydrothermal synthesis of Ficus racemose for therapy, diagnosis, and cell tracking. Reproduced from Ref. [102] with permission from Royal Society of Chemistry.

2.4. Carbon dots (C-DOTs)

C-DOTs can be generally defined as a quasi-0D carbon-based material with a size below 20 nm, and fluorescence is their intrinsic property [103]. C-DOTs, a new rising star in the carbon family, has attracted substantial attention due to their excellent and tunable photoluminescence, high quantum yield, low toxicity, small size, appreciable biocompatibility, and abundant, low-cost sources, providing essential applications in many fields, including biomedicine, catalysis, optoelectronic devices, and anticounterfeiting [104–106].

C-DOTs have been deemed for phototherapy applications, not only as photo absorbing agents but also as nano-carriers. Several hybrids obtained by covalent coupling, electrostatic interaction, or π- π stacking have been tested in the last years [107,108].

2.4.1 Application of C-DOTs in PDT

The antitumor effect of C-DOTs conjugates based for PDT treatment of cancer disease has been confirmed by several authors. Li et al. (2017) prepared porphyrin-containing C-DOTs and evidenced the effective photodynamic activity in hepatoma treatment. Their results showed that the material possesses good photostability, biocompatibility, cellular uptake, and potent cytotoxicity upon irradiation *in vitro* and that *in vivo* can suppress the tumor mass [109]. Huang et al. (2012) prepared a novel theranostic system based on chlorin e6-conjugated C-DOTs. The *in vitro* results determined that the composite upon irradiation exhibit good stability and solubility, low cytotoxicity, good biocompatibility, enhanced photosensitizer fluorescence detection, and remarkable photodynamic efficacy compared to Ce6 alone.

Furthermore, the *in vivo* results suggested that the newly synthesized nanocomposite possesses excellent imaging efficacy [110]. Qin et al. (2021) produced C-DOTs by microplasma using o-phenylenediamine, revealing a broad absorption peak at 380–500 nm and

Preprints (www.preprints.org) | NOT PEER-REVIEWED | Posted: 5 November 2021 doi:10.20944/preprints202111.0119.v1

emitted bright yellow fluorescence with a peak at 550 nm. The C-DOTs were rapidly taken up by HeLa cancer cells. A bright yellow fluorescence signal and intense ROS were efficiently produced when excited under blue light, enabling simultaneous fluorescent cancer cell imaging and photodynamic inactivation, with a 40% decrease in relative cell viability [111].

A simplified scheme of the production of ROS for PDT based on C-DOTs is shown in Figure 8.

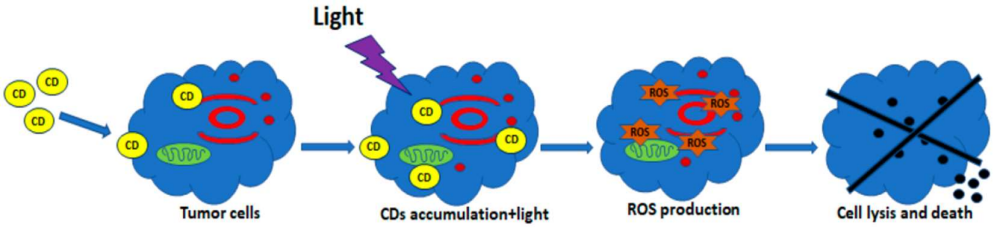

Figure 8. Schematic diagram of photodynamic Therapy. CD (C-DOTs) penetrate the cell membrane and accumulate in the cytosol. Light irradiation actives and induces the production of ROS. Reproduced from Ref. [112] with permission from MPDI.

2.4.2 Application of C-DOTs in PTT

The study of Meena and coworkers (2019) demonstrated that C-DOTs (synthesized from ayurvedic medicinal plants) with a concentration of 0.5 mg/mL and under 10 min of light exposure (750 nm) reached a temperature up to 46°C verifying its potential on photothermal therapy. Besides, no significant toxicity was revealed against NIH-3T3 normal cells, indicating attractive behavior in this field [113]. Sun et al. (2016) demonstrated that red emissive C-DOTs were able to efficiently and quickly convert laser energy into heat and that upon laser irradiation for 10 min, the viability of MCF-7 cells was significantly reduced as the concentration increased (20–200μg/mL) [114]. Geng et al. (2018) showed that NIR-absorbing nitrogen and oxygen co-doped C-DOTs generate high-efficiency heat under laser irradiation at low power density achieving 100% of tumor ablation without causing any side effects [115]. Zheng et al. (2016) synthesized NIR fluorescent (600 nm to 900 nm) composite from a hydrophobic cyanine dye and poly(ethylene glycol) (PEG800) with preferential uptake and accumulation to tumors and high photothermal conversion efficiency (38.7%) as a novel theranostic agent for NIR fluorescent imaging and PTT *in vivo* and *in vitro* [116]

2.4.3 Application of C-DOTs in synergistic therapy

Jia et al. (2018) tested *in vivo*/*in vitro* PDT, and PTT properties of green synthesized C-DOTs against HeLa cells under 635 nm of irradiation, demonstrating 0.38% of quantum yield and 27.6% of photothermal conversion efficiency [117]. It is worth noting that ROS and heat generation are desirable, but also selectivity is essential. For example, besides cancer cells, lysosome targeting has also been assessed, showing promising results [118]. Furthermore, some studies have been published comprising synergistic therapy with multifunctional C-DOTs. So, Lan et al. (2018) synthesized C-DOTs and confirmed their PDT and PTT activities under 800 nm of irradiation. In addition, its fluorescence and photoacoustic properties for imaging were verified [119]. Similar evaluations were carried out by Sun et al. (2019), using amino C-DOTs modified with 0.56% (w/w) of chlorin e6, but with irradiation of 671 nm [120]. In this context, Guo and coworkers (2018) developed Cu, N-doped C-DOTs using different temperatures in a simple hydrothermal method. They evaluated the PDT and PTT capabilities under 808 nm, determining ROS generation and a rise in temperature up to 53 °C [121]. Zhang et al. (2018) synthesized a therapeutic agent DOX loaded, sgc8c aptamer conjugated, and SWCNTs-PEG-Fe3O4@CQDs with multifunction

Preprints (www.preprints.org) | NOT PEER-REVIEWED | Posted: 5 November 2021 doi:10.20944/preprints202111.0119.v1

ability can target and kill cancer cells by releasing the drug photodynamically or photothermally. SWCNTs-PEG-Fe3O4@CQDs convert 808 nm NIR into heat energy, generate ROS (reactive oxygen species), and remove cancer cells. SWCNT-PEG-Fe3O4@CQD nanocarriers are favorable for treating cervical cancer and other diseases that need precise drug targeting [116]. Yang et al. (2019) synthesized C-DOTs/Hemin. The composite could increase the temperature enhancement to ca 26 °C under laser irradiation, with outstanding photo-dynamic efficacy. More than 90% of cancer cells die after 10 min laser treatment. This hybrid showed high ROS generation using DCFH-DA probe against HepG2 cells [122]

A simplified scheme of ROS production for PDT and heat for PTT therapies based on C-DOTs is shown in Figure 9.

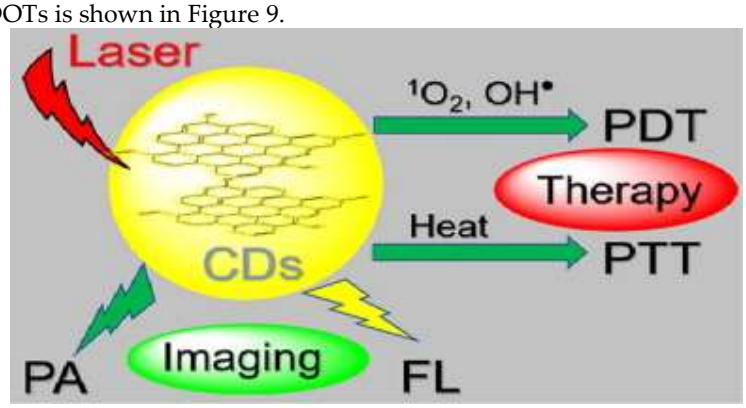

Figure 9. Lysosome targetable C-DOTS, which can simultaneously generate $^1O_2$, OH•, and heat under 635 nm laser irradiation. Reproduced from Ref. [123] with permission from Elsevier

3. Toxicology and immune response of CBM

The interaction of any nanoparticle with biological molecules depends on its physicochemical characteristics. Given the many advantages of CBM, it is also necessary to highlight the possible effects of toxicity. Composition, size, shape, charge, functionalization, and aggregation are some examples of these properties that must be studied and understood to avoid toxic effects. Nanomaterials, especially carbon-based, appear in different shapes and structures, such as particles, tubes, fibers, and films, and this variation directly affects their kinetics and delivery to the target cell. Consequently, the route of transport in the environment is also affected [124].

ROS production is one of the essential mechanisms of toxicity of these nanomaterials and can lead to a chain of reactions ranging from inflammation and oxidative stress to protein denaturation and cell death [125]. This generation of ROS can reduce the membrane potential of mitochondria, causing damage to the cell and can react with fatty acids, causing lipid peroxidation. In the nucleus, CBM can also cause genotoxicity by interacting with DNA. These processes are the main factors related to toxicity and cell death caused by carbon-based nanomaterials [126].

The small size of nanomaterials enables them to cross biological barriers, including membranes, which can lead to cell damage [124]. Smaller CBM has shown greater oxidative capacity and causes more oxidative damage to alveolar epithelial cells than the bigger ones [127]. Regarding graphene-based nanomaterials, GO, for example, due to their size, can cross cell membranes, which can damage them and promote cytoplasmic leakage with the generation of ROS [128]. Also, when the surface area of nanoparticles is large, there is an increase in their binding capacity with other compounds on their surface, increasing their toxic effect in the biological environment. The bigger the surface area of CBM, the greater their oxidative potential, including the ability to damage DNA[129].

Understanding the characteristics of CBM is essential to improving their biocompatibility. For example, carbon nanotubes are hydrophobic and can aggregate in the blood,

and several strategies have been adopted to improve their delivery in the biological environment via the intravenous route [130].

Different ligands should reduce cytotoxicity. In PEG-functionalized GO, no significant changes were observed in the Zebrafish model [131] compared to several already shown effects of GO without PEG. This functionalization improves its solubility and compatibility and has also reduced toxic effects in mice [132]. Intravenous administration of amine-functionalized GO or only GO in mice proved the thrombogenic capacity of graphene, where functionalized graphene showed low toxicity [133]. Functionalization also changed the toxicity of single-wall carbon nanotubes, showing more biocompatibility for the presence of PEG since PEGylation alters its cytotoxic potential and has improved its excretion in animal tests [130].

Functionalization can also help increase specificity since only diseased cells will receive the nanoparticles, reducing toxicity in healthy tissues. Another possibility to improve CBM is their immobilization in a polymer matrix, preventing penetration into the cell and sealing its edges. But these matrices must be very well studied about biocompatibility for human application [128].

It is necessary to understand the process of elimination and metabolism of CBM in the human body to be used in medicine. If they are not eliminated or accumulate in some vital organ, they can pose a health risk and, therefore, studies in this area are critical [130].

The cytotoxicity results of CBM are often contradictory. Not only because the physical-chemical characteristics can influence these results, but the synthesis process itself and the presence of metallic impurities can also influence them. Thus, it is still unclear what plays a central role in the immune response and the toxicity of these nanomaterials [134]. These results are found especially for graphene which structural properties directly influence its interaction with cells. Chemical oxidants and reducing agents used in graphene synthesis can result in organic contamination and metallic impurities, resulting in cell damage and increased toxicity. Carbon nanotubes are considered genotoxic, and this characteristic can be explained both by the fibrous property of these materials and the presence of impurities present in their composition [135]. The use of green synthesis can reduce their cytotoxicity and be a possibility in biomedical applications [128].

It should be noted that the prediction of in vivo toxicity from in vitro data does not necessarily reflect reality due to the different conditions of the cellular environment and the complex organism. But understanding these processes can go a long way in controlling these toxic effects. In vivo studies can provide information about complex parameters such as metabolism and evaluation of the chronic effect, which can contrast with punctual in vitro results. The contradiction in the toxicity of the same compound may also result from these differences [124]. The poor dispersion of CBM in water also plays an essential role in the toxicity and reproducibility of both in vitro and in vivo assays [136].

CBM absorbs over a broad region of the visible spectrum and can directly interfere in assays performed by fluorescence or absorption. Thus, the inconsistency concerning toxicity can still result from a technical inconsistency in the reading of toxicity tests with the use of CBM. Therefore, it is necessary to characterize these materials, especially regarding the reproducibility of toxicological tests. Ensuring the reproducibility of the technique itself, the better characterized, the less toxic effects are found, significantly as they are easily modified. Removing metallic impurities, adding binders on its surface, or increasing its dispersion are examples of processes with apparent effectiveness in producing less toxic materials [134].

Graphene and carbon nanotubes have different geometries. While the last one is shaped like a tube, as the name implies, the first one is formed by flat sheets. Thus, the interaction of these materials with the biological environment must happen through different mechanisms and, therefore, result in different responses, including specific toxicity and immunological effects [130]. Dose, interaction time, cell type, and animal lineage can influence the toxicity result [128].

The route of administration, such as oral, intraperitoneal, intravenous, or ocular, also interferes with the toxicity of CBM [137]. For example, studies have shown few toxic effects

 doi:10.20944/preprints202111.0119.v1

of graphene-based compounds on intraocular administration, with minimal effect on morphology and cell viability [138]. In comparison, studies have shown that graphene can induce chronic toxicity in mice from oral or systemic administration [128]. Pulmonary toxicity with multiple effects has also been reported, depending on the dose of graphene administered [132]. This way also affects the toxicity of carbon nanotubes. Lung exposure leads to different effects, including genotoxic and intravenous injection has resulted in carbon nanotubes accumulation in vital organs. But these responses are mainly dependent on dose, functionalization, and physicochemical properties [139].

Graphene toxicity was shown to be dose-dependent, as it had significant effects at high doses in mice (such as inflammation and pulmonary edema), whereas it exhibited little or no effect at low and medium doses. Therefore, it is necessary to avoid general conclusions regarding these CBM. Understanding the biological interaction of the compounds (functionalized or not) can guarantee better results and may be the key to them being considered non-toxic [132].

Different compounds can interact with immune cells and trigger a response. As for toxicity, carbon-based compounds can act differently depending on their properties, such as size, shape, dispersion, and different functionalization [134].

Macrophage tests are the most used to study the immune response of these materials. Studies with cell uptake and viability and induction of an inflammatory response are some examples of these tests. Especially in macrophages, CBM has been exhibiting detrimental effects. But nanoparticle size may be definitive for the answer since, for example, short and long carbon nanotubes can show different answers. Another essential cell for the immune response is lymphocytes. CBM has been studied and has both a positive and negative effect on modulating the cellular response of lymphocytes, also showing toxicity of these materials [134].

There are several in vitro toxicity studies with carbon nanotubes, especially in lung and skin cells and cells related to the immune system. Most have been showing decreases in cell proliferation, which can reduce the adhesion of carbon nanotubes, generating a series of reactions that will damage the membranes and cause cell death. Other studies have shown the potential for DNA damage and genetic alterations in carbon nanotubes [139].

In addition to the individual in vitro responses, in vivo tests allow studying the global immune response of compounds in the living organism from a systemic response. Studies with alveolar macrophages, inflammatory induction in the lungs, airway epithelial cells, and mast cells are some examples of what has been studied with CBM. Systemic activation of the immune response and the complement system are also possible with the in vivo study. Carbon nanotubes, for example, can activate this systemic response [134].

The use of high doses, the lack of standardization, exposure to professionals, and the effect on the environment are some examples of the origin of these problems. The development of regulations, whether in the production or disposal of these materials, is an essential step in reducing the adverse effects of nanomaterials and has been a concern of the global scientific community [124]. The influence of graphene on plantations has shown that it can induce adverse effects, including on plantation roots, being dose-dependent. The structure can also be a determining factor, as few layers did not significantly affect plant growth rates. Furthermore, high concentrations of graphene can affect microorganisms in the environment, including water, affecting plant growth and the general biome. Therefore, understanding toxicity must be a constant concern for those working with these compounds [132].

CBM has wide applications. However, before applying these materials for any research, it is necessary to study and understand their toxic effects, mainly because they often allow for modifications and reductions in toxicity, making them even more attractive for use in nanomedicine.

4. Conclusions

Based on the compilation prepared in this mini-review, it is evident that a wide range of carbon-based materials are being used within phototherapy and synergetic therapies to battle against cancer disease. Graphene oxide, reduced GO, graphene quantum dots, and carbon dots have been studied by several researchers showing excellent results for tumor destruction. Nevertheless, it is necessary to define standard guidelines for preparing and applying this type of material within therapeutics. The researchers must employ more and deep in vivo and in vitro tests to scale this application to humans and analyze their response.Worth noting that the phototherapy field is still in an emerging phase. Therefore, further exploration remains to be done until fully high-quality implementation and commercialization. A grand challenge is to develop a treatment with reduced dose-dependent toxicity to improve the care of cancer patients.

Author Contributions: Conceptualization M.P.R.; writing, K.J.L, H.H.B. and M.P.R. All authors have read and agreed to the published version of the manuscript.

Funding: This research received no external funding.

Data Availability Statement: Not applicable.

Acknowledgments: Financial support from FAPESP (Fundação de Amparo à Pesquisa do Estado de São Paulo) grants 2013/07276-1 and 2016/14033-6. Escuela Politécnica Nacional Project PIIF-20-05

Conflicts of Interest: The authors declare no conflict of interest.

References

1. Hohlfeld, B.F.; Gitter, B.; Flanagan, K.J.; Kingsbury, C.J.; Kulak, N.; Senge, M.O.; Wiehe, A. Exploring the relationship between structure and activity in BODIPYs designed for antimicrobial phototherapy. *Org. Biomol. Chem.* **2020**, *18*, 2416–2431, doi:10.1039/d0ob00188k.
2. Zhou, S.; Wang, Z.; Wang, Y.; Feng, L. Near-Infrared Light-Triggered Synergistic Phototherapy for Antimicrobial Therapy. *ACS Appl. Bio Mater.* **2020**, *3*, 1730–1737, doi:10.1021/acsabm.0c00034.
3. Gwynne, P.J.; Gallagher, M.P. Light as a broad-spectrum antimicrobial. *Front. Microbiol.* **2018**, *9*, 1–9, doi:10.3389/fmicb.2018.00119.
4. Zubair, R.; Hamzavi, I.H. Phototherapy for Vitiligo. *Dermatol. Clin.* **2020**, *38*, 55–62, doi:10.1016/j.det.2019.08.005.
5. Morita, A. Current developments in phototherapy for psoriasis. *J. Dermatol.* **2018**, *45*, 287–292, doi:10.1111/1346-8138.14213.
6. Kemény, L.; Varga, E.; Novak, Z. Advances in phototherapy for psoriasis and atopic dermatitis. *Expert Rev. Clin. Immunol.* **2019**, *15*, 1205–1214, doi:10.1080/1744666X.2020.1672537.
7. Nikolaou, V.; Sachlas, A.; Papadavid, E.; Economidi, A.; Karambidou, K.; Marinos, L.; Stratigos, A.; Antoniou, C. Phototherapy as a first-line treatment for early-stage mycosis fungoides: The results of a large retrospective analysis. *Photodermatol. Photoimmunol. Photomed.* **2018**, *34*, 307–313, doi:10.1111/phpp.12383.
8. Cao, J.; Chen, Z.; Chi, J.; Sun, Y.; Sun, Y. Recent progress in synergistic chemotherapy and phototherapy by targeted drug delivery systems for cancer treatment. *Artif. Cells, Nanomedicine Biotechnol.* **2018**, *46*, 817–830, doi:10.1080/21691401.2018.1436553.
9. Zhen, X.; Cheng, P.; Pu, K. Recent Advances in Cell Membrane–Camouflaged Nanoparticles for Cancer Phototherapy. *Small* **2019**, *15*, 1–19, doi:10.1002/smll.201804105.
10. Ma, Y.; Zhang, Y.; Li, X.; Zhao, Y.; Li, M.; Jiang, W.; Tang, X.; Dou, J.; Lu, L.; Wang, F.; et al. Near-infrared II phototherapy induces deep tissue immunogenic cell death and potentiates cancer immunotherapy. *ACS Nano* **2019**, *13*, 11967–11980, doi:10.1021/acsnano.9b06040.
11. Xie, Z.; Fan, T.; An, J.; Choi, W.; Duo, Y.; Ge, Y.; Zhang, B.; Nie, G.; Xie, N.; Zheng, T.; et al. Emerging combination strategies with phototherapy in cancer nanomedicine. *Chem. Soc. Rev.* **2020**, doi:10.1039/d0cs00215a.
12. Sun, W.; Zhao, X.; Fan, J.; Du, J.; Peng, X. Boron Dipyrromethene Nano-Photosensitizers for Anticancer Phototherapies. *Small* **2019**, *15*, 1–25, doi:10.1002/smll.201804927.
13. Ng, C.W.; Li, J.; Pu, K. Recent Progresses in Phototherapy-Synergized Cancer Immunotherapy. *Adv. Funct. Mater.* **2018**, *28*, 1–20, doi:10.1002/adfm.201804688.
14. Zhang, S.; Li, Q.; Yang, N.; Shi, Y.; Ge, W.; Wang, W.; Huang, W.; Song, X.; Dong, X. Phase-Change Materials Based Nanoparticles for Controlled Hypoxia Modulation and Enhanced Phototherapy. *Adv. Funct. Mater.* **2019**, *29*, 1–9,

doi:10.1002/adfm.201906805.

15. Li, J.; Pu, K. Development of organic semiconducting materials for deep-tissue optical imaging, phototherapy and photoactivation. *Chem. Soc. Rev.* **2019**, *48*, 38–71, doi:10.1039/c8cs00001h.
16. Wang, Y.; Jin, Y.; Chen, W.; Wang, J.; Chen, H.; Sun, L.; Li, X.; Ji, J.; Yu, Q.; Shen, L.; et al. Construction of nanomaterials with targeting phototherapy properties to inhibit resistant bacteria and biofilm infections. *Chem. Eng. J.* **2019**, *358*, 74–90, doi:10.1016/j.cej.2018.10.002.
17. Lan, G.; Ni, K.; Lin, W. Nanoscale metal–organic frameworks for phototherapy of cancer. *Coord. Chem. Rev.* **2019**, *379*, 65–81, doi:https://doi.org/10.1016/j.ccr.2017.09.007.
18. Jung, H.S.; Verwilst, P.; Sharma, A.; Shin, J.; Sessler, J.L.; Kim, J.S. Organic molecule-based photothermal agents: An expanding photothermal therapy universe. *Chem. Soc. Rev.* **2018**, *47*, 2280–2297, doi:10.1039/c7cs00522a.
19. Liu, Y.; Bhattarai, P.; Dai, Z.; Chen, X. Photothermal therapy and photoacoustic imaging: Via nanotheranostics in fighting cancer. *Chem. Soc. Rev.* **2019**, *48*, 2053–2108, doi:10.1039/c8cs00618k.
20. Nafiujjaman, M.; Nurunnabi, M. *Graphene and 2D Materials for Phototherapy*; Elsevier Inc., 2019; ISBN 9780128158890.
21. Del Rosal, B.; Jia, B.; Jaque, D. Beyond Phototherapy: Recent Advances in Multifunctional Fluorescent Nanoparticles for Light-Triggered Tumor Theranostics. *Adv. Funct. Mater.* 2018, *28*, 1–25.
22. Wang, Y.; Jin, Y.; Chen, W.; Wang, J.; Chen, H.; Sun, L.; Li, X.; Ji, J.; Yu, Q.; Shen, L.; et al. Construction of nanomaterials with targeting phototherapy properties to inhibit resistant bacteria and biofilm infections. *Chem. Eng. J.* **2019**, *358*, 74–90, doi:10.1016/j.cej.2018.10.002.
23. Wiehe, A.; O'brien, J.M.; Senge, M.O. Trends and targets in antiviral phototherapy. *Photochem. Photobiol. Sci.* **2019**, *18*, 2565–2612, doi:10.1039/c9pp00211a.
24. Rajakumar, G.; Zhang, X.H.; Gomathi, T.; Wang, S.F.; Ansari, M.A.; Mydhili, G.; Nirmala, G.; Alzohairy, M.A.; Chung, I.M. Current use of carbon-based materials for biomedical applications-A prospective and review. *Processes* **2020**, *8*, 1–16, doi:10.3390/PR8030355.
25. Lu, D.; Tao, R.; Wang, Z. Carbon-based materials for photodynamic therapy: A mini-review. *Front. Chem. Sci. Eng.* **2019**, *13*, 310–323, doi:10.1007/s11705-018-1750-7.
26. Zhu, H.; Ni, N.; Govindarajan, S.; Ding, X.; Leong, D.T. Phototherapy with layered materials derived quantum dots. *Nanoscale* **2020**, *12*, 43–57, doi:10.1039/c9nr07886j.
27. Jiang, B.P.; Zhou, B.; Lin, Z.; Liang, H.; Shen, X.C. Recent Advances in Carbon Nanomaterials for Cancer Phototherapy. *Chem. - A Eur. J.* **2019**, *25*, 3993–4004, doi:10.1002/chem.201804383.
28. Abbas, A.; Mariana, L.T.; Phan, A.N. Biomass-waste derived graphene quantum dots and their applications. *Carbon N. Y.* **2018**, *140*, 77–99, doi:10.1016/j.carbon.2018.08.016.
29. Lian, Y.M.; Utetiwabo, W.; Zhou, Y.; Huang, Z.H.; Zhou, L.; Muhammad, F.; Chen, R.J.; Yang, W. From upcycled waste polyethylene plastic to graphene/mesoporous carbon for high-voltage supercapacitors. *J. Colloid Interface Sci.* **2019**, *557*, 55–64, doi:10.1016/j.jcis.2019.09.003.
30. Lee, X.J.; Hiew, B.Y.Z.; Lai, K.C.; Lee, L.Y.; Gan, S.; Thangalazhy-Gopakumar, S.; Rigby, S. Review on graphene and its derivatives: Synthesis methods and potential industrial implementation. *J. Taiwan Inst. Chem. Eng.* **2019**, *98*, 163–180, doi:10.1016/j.jtice.2018.10.028.
31. Lim, J.Y.; Mubarak, N.M.; Abdullah, E.C.; Nizamuddin, S.; Khalid, M.; Inamuddin Recent trends in the synthesis of graphene and graphene oxide based nanomaterials for removal of heavy metals — A review. *J. Ind. Eng. Chem.* **2018**, *66*, 29–44, doi:10.1016/j.jiec.2018.05.028.
32. Kumar, A.; Sharma, K.; Dixit, A.R. A review of the mechanical and thermal properties of graphene and its hybrid polymer nanocomposites for structural applications. *J. Mater. Sci.* **2019**, *54*, 5992–6026, doi:10.1007/s10853-018-03244-3.
33. Mohan, V.B.; Lau, K. tak; Hui, D.; Bhattacharyya, D. Graphene-based materials and their composites: A review on production, applications and product limitations. *Compos. Part B Eng.* **2018**, *142*, 200–220, doi:10.1016/j.compositesb.2018.01.013.
34. Wang, R.; Ren, X.G.; Yan, Z.; Jiang, L.J.; Sha, W.E.I.; Shan, G.C. Graphene based functional devices: A short review. *Front. Phys.* **2019**, *14*, 9–18, doi:10.1007/s11467-018-0859-y.
35. Zhu, Y.; Ji, H.; Cheng, H.M.; Ruoff, R.S. Mass production and industrial applications of graphene materials. *Natl. Sci. Rev.* **2018**, *5*, 90–101, doi:10.1093/nsr/nwx055.
36. Banerjee, A.N. Graphene and its derivatives as biomedical materials: Future prospects and challenges. *Interface Focus* **2018**, *8*, doi:10.1098/rsfs.2017.0056.
37. Seifi, T.; Reza Kamali, A. Antiviral performance of graphene-based materials with emphasis on COVID-19: A review. *Med. Drug Discov.* **2021**, *11*, 100099, doi:10.1016/j.medidd.2021.100099.
38. Karahan, H.E.; Wiraja, C.; Xu, C.; Wei, J.; Wang, Y.; Wang, L.; Liu, F.; Chen, Y. Graphene Materials in Antimicrobial Nanomedicine: Current Status and Future Perspectives. *Adv. Healthc. Mater.* **2018**, *7*, 1–18, doi:10.1002/adhm.201701406.
39. Sainz-urruela, C.; Vera-lópez, S.; Andrés, M.P.S.; Díez-pascual, A.M. Graphene-based sensors for the detection of bioactive compounds: A review. *Int. J. Mol. Sci.* **2021**, *22*, doi:10.3390/ijms22073316.
40. Yang, K.; Feng, L.; Liu, Z. The advancing uses of nano-graphene in drug delivery. *Expert Opin. Drug Deliv.* **2015**, *12*, 601–612, doi:10.1517/17425247.2015.978760.

41. Lin, J.; Huang, Y.; Huang, P. Graphene-Based Nanomaterials in Bioimaging. In *Biomedical Applications of Functionalized Nanomaterials: Concepts, Development and Clinical Translation*; Elsevier Inc., 2018; pp. 247–287 ISBN 9780323508797.
42. Shin, S.R.; Li, Y.C.; Jang, H.L.; Khoshakhlagh, P.; Akbari, M.; Nasajpour, A.; Zhang, Y.S.; Tamayol, A.; Khademhosseini, A. Graphene-based materials for tissue engineering. *Adv. Drug Deliv. Rev.* **2016**, *105*, 255–274, doi:10.1016/j.addr.2016.03.007.
43. Patel, S.C.; Lee, S.; Lalwani, G.; Suhrland, C.; Chowdhury, S.M.; Sitharaman, B. Graphene-based platforms for cancer therapeutics. *Ther. Deliv.* **2016**, *7*, 101–116, doi:10.4155/tde.15.93.
44. Yang, K.; Feng, L.; Zhuang, L. Stimuli responsive drug delivery systems based on nano-graphene for cancer therapy. *Adv. Drug Deliv. Rev.* **2016**, *105*, 228–241, doi:10.1016/j.addr.2016.05.015.
45. Romero, M.P.; Marangoni, V.S.; de Faria, C.G.; Leite, I.S.; Silva, C. de C.C. e.; Maroneze, C.M.; Pereira-da-Silva, M.A.; Bagnato, V.S.; Inada, N.M. Graphene Oxide Mediated Broad-Spectrum Antibacterial Based on Bimodal Action of Photodynamic and Photothermal Effects. *Front. Microbiol.* **2020**, *10*, 1–15, doi:10.3389/fmicb.2019.02995.
46. Chen, Y.W.; Su, Y.L.; Hu, S.H.; Chen, S.Y. Functionalized graphene nanocomposites for enhancing photothermal therapy in tumor treatment. *Adv. Drug Deliv. Rev.* **2016**, *105*, 190–204, doi:10.1016/j.addr.2016.05.022.
47. Melios, C.; Giusca, C.E.; Panchal, V.; Kazakova, O. Water on graphene: Review of recent progress. *2D Mater.* **2018**, *5*, doi:10.1088/2053-1583/aa9ea9.
48. Tadyszak, K.; Wychowaniec, J.K.; Litowczenko, J. Biomedical applications of graphene-based structures. *Nanomaterials* **2018**, *8*, 1–20, doi:10.3390/nano8110944.
49. Dasari Shareena, T.P.; McShan, D.; Dasmahapatra, A.K.; Tchounwou, P.B. A Review on Graphene-Based Nanomaterials in Biomedical Applications and Risks in Environment and Health. *Nano-Micro Lett.* **2018**, *10*, 1–34, doi:10.1007/s40820-018-0206-4.
50. Molaei, M.J. Carbon quantum dots and their biomedical and therapeutic applications: A review. *RSC Adv.* **2019**, *9*, 6460–6481, doi:10.1039/c8ra08088g.
51. Yan, F.; Jiang, Y.; Sun, X.; Bai, Z.; Zhang, Y.; Zhou, X. Surface modification and chemical functionalization of carbon dots: a review. *Microchim. Acta* **2018**, *185*, doi:10.1007/s00604-018-2953-9.
52. Tian, P.; Tang, L.; Teng, K.S.; Lau, S.P. Graphene quantum dots from chemistry to applications. *Mater. Today Chem.* **2018**, *10*, 221–258, doi:10.1016/j.mtchem.2018.09.007.
53. Costa, M.C.F.; Marangoni, V.S.; Ng, P.R.; Nguyen, H.T.L.; Carvalho, A.; Castro Neto, A.H. Accelerated synthesis of graphene oxide from graphene. *Nanomaterials* **2021**, *11*, 1–8, doi:10.3390/nano11020551.
54. Singh, D.P.; Herrera, C.E.; Singh, B.; Singh, S.; Singh, R.K.; Kumar, R. Graphene oxide: An efficient material and recent approach for biotechnological and biomedical applications. *Mater. Sci. Eng. C* **2018**, *86*, 173–197, doi:10.1016/j.msec.2018.01.004.
55. Smith, A.T.; LaChance, A.M.; Zeng, S.; Liu, B.; Sun, L. Synthesis, properties, and applications of graphene oxide/reduced graphene oxide and their nanocomposites. *Nano Mater. Sci.* **2019**, *1*, 31–47, doi:10.1016/j.nanoms.2019.02.004.
56. Justh, N.; Berke, B.; László, K.; Szilágyi, I.M. Thermal analysis of the improved Hummers' synthesis of graphene oxide. *J. Therm. Anal. Calorim.* **2018**, *131*, 2267–2272, doi:10.1007/s10973-017-6697-2.
57. Sharma, H.; Mondal, S. Functionalized graphene oxide for chemotherapeutic drug delivery and cancer treatment: A promising material in nanomedicine. *Int. J. Mol. Sci.* **2020**, *21*, 1–42, doi:10.3390/ijms21176280.
58. Liu, L.; Ma, Q.; Cao, J.; Gao, Y.; Han, S.; Liang, Y.; Zhang, T.; Song, Y.; Sun, Y. Recent progress of graphene oxide-based multifunctional nanomaterials for cancer treatment. *Cancer Nanotechnol.* **2021**, *12*, 1–31, doi:10.1186/s12645-021-00087-7.
59. Hosseinzadeh, R.; Khorsandi, K.; Hosseinzadeh, G. Graphene oxide-methylene blue nanocomposite in photodynamic therapy of human breast cancer. *J. Biomol. Struct. Dyn.* **2018**, *36*, 2216–2223, doi:10.1080/07391102.2017.1345698.
60. Sun, X.; Zebibula, A.; Dong, X.; Zhang, G.; Zhang, D.; Qian, J.; He, S. Aggregation-Induced Emission Nanoparticles Encapsulated with PEGylated Nano Graphene Oxide and Their Applications in Two-Photon Fluorescence Bioimaging and Photodynamic Therapy in Vitro and in Vivo. *ACS Appl. Mater. Interfaces* **2018**, *10*, 25037–25046, doi:10.1021/acsami.8b05546.
61. Qin, X.; Zhang, H.; Wang, Z.; Jin, Y. Magnetic chitosan/graphene oxide composite loaded with novel photosensitizer for enhanced photodynamic therapy. *RSC Adv.* **2018**, *8*, 10376–10388, doi:10.1039/c8ra00747k.
62. Huang, P.; Xu, C.; Lin, J.; Wang, C.; Wang, X.; Zhang, C.; Zhou, X.; Guo, S.; Cui, D. Folic Acid-conjugated Graphene Oxide loaded with Photosensitizers for Targeting Photodynamic Therapy. *Theranostics* **2012**, *1*, 240–250, doi:10.7150/thno/v01p0240.
63. Patil, T. V.; Patel, D.K.; Dutta, S.D.; Ganguly, K.; Lim, K.T. Graphene oxide-based stimuli-responsive platforms for biomedical applications. *Molecules* **2021**, *26*, 1–19, doi:10.3390/molecules26092797.
64. Lim, J.H.; Kim, D.E.; Kim, E.J.; Ahrberg, C.D.; Chung, B.G. Functional Graphene Oxide-Based Nanosheets for Photothermal Therapy. *Macromol. Res.* **2018**, *26*, 557–565, doi:10.1007/s13233-018-6067-3.
65. Xie, M.; Zhang, F.; Peng, H.; Zhang, Y.; Li, Y.; Xu, Y.; Xie, J. Layer-by-layer modification of magnetic graphene oxide by chitosan and sodium alginate with enhanced dispersibility for targeted drug delivery and photothermal therapy. *Colloids Surfaces B Biointerfaces* **2019**, *176*, 462–470, doi:https://doi.org/10.1016/j.colsurfb.2019.01.028.
66. Huang, C.; Hu, X.; Hou, Z.; Ji, J.; Li, Z.; Luan, Y. Tailored graphene oxide-doxorubicin nanovehicles via near-infrared dye-lactobionic acid conjugates for chemo-photothermal therapy. *J. Colloid Interface Sci.* **2019**, *545*, 172–183, doi:https://doi.org/10.1016/j.jcis.2019.03.019.

67. Zhang, W.; Guo, Z.; Huang, D.; Liu, Z.; Guo, X.; Zhong, H. Synergistic effect of chemo-photothermal therapy using PEGylated graphene oxide. *Biomaterials* **2011**, *32*, 8555–8561, doi:10.1016/j.biomaterials.2011.07.071.
68. Gulzar, A.; Xu, J.; Yang, D.; Xu, L.; He, F.; Gai, S.; Yang, P. Nano-graphene oxide-UCNP-Ce6 covalently constructed nanocomposites for NIR-mediated bioimaging and PTT/PDT combinatorial therapy. *Dalt. Trans.* **2018**, *47*, 3931–3939, doi:10.1039/c7dt04141a.
69. Zhang, X.; Luo, L.; Li, L.; He, Y.; Cao, W.; Liu, H.; Niu, K.; Gao, D. Trimodal synergistic antitumor drug delivery system based on graphene oxide. *Nanomedicine Nanotechnology, Biol. Med.* **2019**, *15*, 142–152, doi:10.1016/j.nano.2018.09.008.
70. Romero, M.P.; Buzza, H.H.; Stringasci, M.D.; Estevão, B.M.; Silva, C.C.C.; Pereira-Da-silva, M.A.; Inada, N.M.; Bagnato, V.S. Graphene oxide theranostic effect: Conjugation of photothermal and photodynamic therapies based on an in vivo demonstration. *Int. J. Nanomedicine* **2021**, *16*, 1601–1616, doi:10.2147/IJN.S287415.
71. Coros, M.; Pogacean, F.; Turza, A.; Dan, M.; Berghian-Grosan, C.; Pana, I.O.; Pruneanu, S. Green synthesis, characterization and potential application of reduced graphene oxide. *Phys. E Low-Dimensional Syst. Nanostructures* **2020**, *119*, 113971, doi:10.1016/j.physe.2020.113971.
72. Muzyka, R.; Drewniak, S.; Pustelny, T.; Chrubasik, M.; Gryglewicz, G. Characterization of graphite oxide and reduced graphene oxide obtained from different graphite precursors and oxidized by different methods using Raman spectroscopy. *Materials (Basel).* **2018**, *11*, 15–17, doi:10.3390/ma11071050.
73. Tarcan, R.; Todor-Boer, O.; Petrovai, I.; Leordean, C.; Astilean, S.; Botiz, I. Reduced graphene oxide today. *J. Mater. Chem. C* **2020**, *8*, 1198–1224, doi:10.1039/c9tc04916a.
74. Dash, B.S.; Jose, G.; Lu, Y.J.; Chen, J.P. Functionalized reduced graphene oxide as a versatile tool for cancer therapy. *Int. J. Mol. Sci.* **2021**, *22*, 1–24, doi:10.3390/ijms22062989.
75. Kapri, S.; Bhattacharyya, S. Molybdenum sulfide-reduced graphene oxide p-n heterojunction nanosheets with anchored oxygen generating manganese dioxide nanoparticles for enhanced photodynamic therapy. *Chem. Sci.* **2018**, *9*, 8982–8989, doi:10.1039/c8sc02508h.
76. Vinothini, K.; Rajendran, N.K.; Rajan, M.; Ramu, A.; Marraiki, N.; Elgorban, A.M. A magnetic nanoparticle functionalized reduced graphene oxide-based drug carrier system for a chemo-photodynamic cancer therapy. *New J. Chem.* **2020**, *44*, 5265–5277, doi:10.1039/d0nj00049c.
77. Jafarirad, S.; Hammami Torghabe, E.; Rasta, S.H.; Salehi, R. A novel non-invasive strategy for low-level laser-induced cancer therapy by using new Ag/ZnO and Nd/ZnO functionalized reduced graphene oxide nanocomposites. *Artif. Cells, Nanomedicine Biotechnol.* **2018**, *46*, 800–816, doi:10.1080/21691401.2018.1470523.
78. Lima-Sousa, R.; de Melo-Diogo, D.; Alves, C.G.; Costa, E.C.; Ferreira, P.; Louro, R.O.; Correia, I.J. Hyaluronic acid functionalized green reduced graphene oxide for targeted cancer photothermal therapy. *Carbohydr. Polym.* **2018**, *200*, 93–99, doi:10.1016/j.carbpol.2018.07.066.
79. de Paula, R.F.O.; Rosa, I.A.; Gafanhão, I.F.M.; Fachi, J.L.; Melero, A.M.G.; Roque, A.O.; Boldrini, V.O.; Ferreira, L.A.B.; Irazusta, S.P.; Ceragioli, H.J.; et al. Reduced graphene oxide, but not carbon nanotubes, slows murine melanoma after thermal ablation using LED light in B16F10 lineage cells. *Nanomedicine Nanotechnology, Biol. Med.* **2020**, *28*, 102231, doi:10.1016/j.nano.2020.102231.
80. Liu, W.; Zhang, X.; Zhou, L.; Shang, L.; Su, Z. Reduced graphene oxide (rGO) hybridized hydrogel as a near-infrared (NIR)/pH dual-responsive platform for combined chemo-photothermal therapy. *J. Colloid Interface Sci.* **2019**, *536*, 160–170, doi:10.1016/j.jcis.2018.10.050.
81. Zaharie-Butucel, D.; Potara, M.; Suarasan, S.; Licarete, E.; Astilean, S. Efficient combined near-infrared-triggered therapy: Phototherapy over chemotherapy in chitosan-reduced graphene oxide-IR820 dye-doxorubicin nanoplatforms. *J. Colloid Interface Sci.* **2019**, *552*, 218–229, doi:10.1016/j.jcis.2019.05.050.
82. Wang, L.; Wang, M.; Zhou, B.; Zhou, F.; Murray, C.; Towner, R.A.; Smith, N.; Saunders, D.; Xie, G.; Chen, W.R. PEGylated reduced-graphene oxide hybridized with Fe3O4 nanoparticles for cancer photothermal-immunotherapy. *J. Mater. Chem. B* **2019**, *7*, 7406–7414, doi:10.1039/c9tb00630c.
83. Zhang, D.Y.; Zheng, Y.; Tan, C.P.; Sun, J.H.; Zhang, W.; Ji, L.N.; Mao, Z.W. Graphene Oxide Decorated with Ru(II)-Polyethylene Glycol Complex for Lysosome-Targeted Imaging and Photodynamic/Photothermal Therapy. *ACS Appl. Mater. Interfaces* **2017**, *9*, 6761–6771, doi:10.1021/acsami.6b13808.
84. Zhang, X.; Wei, C.; Li, Y.; Yu, D. Shining luminescent graphene quantum dots: Synthesis, physicochemical properties, and biomedical applications. *TrAC - Trends Anal. Chem.* **2019**, *116*, 109–121, doi:10.1016/j.trac.2019.03.011.
85. Wu, D.; Liu, Y.; Wang, Y.; Hu, L.; Ma, H.; Wang, G.; Wei, Q. Label-free Electrochemiluminescent Immunosensor for Detection of Prostate Specific Antigen based on Aminated Graphene Quantum Dots and Carboxyl Graphene Quantum Dots. *Sci. Rep.* **2016**, *6*, 1–7, doi:10.1038/srep20511.
86. Tang, L.; Ji, R.; Li, X.; Bai, G.; Liu, C.P.; Hao, J.; Lin, J.; Jiang, H.; Teng, K.S.; Yang, Z.; et al. Deep ultraviolet to near-infrared emission and photoresponse in layered n-doped graphene quantum dots. *ACS Nano* **2014**, *8*, 6312–6320, doi:10.1021/nn501796r.
87. Rakovich, A. Nanomaterials for biosensing and phototherapy applications. *Proc. - Int. Conf. Laser Opt. 2018, ICLO 2018* **2018**, 540, doi:10.1109/LO.2018.8435651.

88. Jiang, C.; Zhao, H.; Xiao, H.; Wang, Y.; Liu, L.; Chen, H.; Shen, C.; Zhu, H.; Liu, Q. Recent advances in graphene-family nanomaterials for effective drug delivery and phototherapy. *Expert Opin. Drug Deliv.* **2020**, *0*, doi:10.1080/17425247.2020.1798400.
89. Henna, T.K.; Pramod, K. Graphene quantum dots redefine nanobiomedicine. *Mater. Sci. Eng. C* **2020**, *110*, doi:10.1016/j.msec.2020.110651.
90. Zheng, X.T.; Ananthanarayanan, A.; Luo, K.Q.; Chen, P. Glowing Graphene Quantum Dots and Carbon Dots: Properties, Syntheses, and Biological Applications. *Small* **2015**, *11*, 1620–1636, doi:https://doi.org/10.1002/smll.201402648.
91. Ge, J.; Lan, M.; Zhou, B.; Liu, W.; Guo, L.; Wang, H.; Jia, Q.; Niu, G.; Huang, X.; Zhou, H.; et al. A graphene quantum dot photodynamic therapy agent with high singlet oxygen generation. *Nat. Commun.* **2014**, *5*, 1–8, doi:10.1038/ncomms5596.
92. Tabish, T.A.; Scotton, C.J.; J Ferguson, D.C.; Lin, L.; Der Veen, A. Van; Lowry, S.; Ali, M.; Jabeen, F.; Winyard, P.G.; Zhang, S. Biocompatibility and toxicity of graphene quantum dots for potential application in photodynamic therapy. *Nanomedicine* **2018**, *13*, 1923–1937, doi:10.2217/nnm-2018-0018.
93. Campbell, E.; Hasan, M.T.; Gonzalez-Rodriguez, R.; Truly, T.; Lee, B.H.; Green, K.N.; Akkaraju, G.; Naumov, A. V. Graphene quantum dot formulation for cancer imaging and redox-based drug delivery. *Nanomedicine Nanotechnology, Biol. Med.* **2021**, *37*, 102408, doi:10.1016/j.nano.2021.102408.
94. Khomidkhodza Kholikova, Saidjafarzoda Ilhoma, Muhammed Sajjada, M.E.S.; Jerry D. Monroeb, Omer Sanc, A.O.E. Improved singlet oxygen generation and antimicrobial activity of sulphur-doped graphene quantum dots coupled with methylene blue for photodynamic therapy applications. *Photodiagnosis Photodyn. Ther.* **2018**, *24*, 7–14, doi:10.1016/j.pdpdt.2018.08.011.
95. Fan, H. yang; Yu, X. hua; Wang, K.; Yin, Y. jia; Tang, Y. jie; Tang, Y. ling; Liang, X. hua Graphene quantum dots (GQDs)-based nanomaterials for improving photodynamic therapy in cancer treatment. *Eur. J. Med. Chem.* **2019**, *182*, 111620, doi:10.1016/j.ejmech.2019.111620.
96. Liu, H.; Li, C.; Qian, Y.; Hu, L.; Fang, J.; Tong, W.; Nie, R.; Chen, Q.; Wang, H. Magnetic-induced graphene quantum dots for imaging-guided photothermal therapy in the second near-infrared window. *Biomaterials* **2020**, *232*, 119700, doi:10.1016/j.biomaterials.2019.119700.
97. Yao, X.; Niu, X.; Ma, K.; Huang, P.; Grothe, J.; Kaskel, S.; Zhu, Y. Graphene Quantum Dots-Capped Magnetic Mesoporous Silica Nanoparticles as a Multifunctional Platform for Controlled Drug Delivery, Magnetic Hyperthermia, and Photothermal Therapy. *Small* **2017**, *13*, 1602225, doi:https://doi.org/10.1002/smll.201602225.
98. Li, S.; Zhou, S.; Li, Y.; Li, X.; Zhu, J.; Fan, L.; Yang, S. Exceptionally High Payload of the IR780 Iodide on Folic Acid-Functionalized Graphene Quantum Dots for Targeted Photothermal Therapy. *ACS Appl. Mater. Interfaces* **2017**, *9*, 22332–22341, doi:10.1021/acsami.7b07267.
99. Wang, H.; Mu, Q.; Wang, K.; Revia, R.A.; Yen, C.; Gu, X.; Tian, B.; Liu, J.; Zhang, M. Nitrogen and boron dual-doped graphene quantum dots for near-infrared second window imaging and photothermal therapy. *Appl. Mater. Today* **2019**, *14*, 108–117, doi:10.1016/j.apmt.2018.11.011.
100. Wang, C.; Chen, Y.; Xu, Z.; Chen, B.; Zhang, Y.; Yi, X.; Li, J. Fabrication and characterization of novel cRGD modified graphene quantum dots for chemo-photothermal combination therapy. *Sensors Actuators, B Chem.* **2020**, *309*, 127732, doi:10.1016/j.snb.2020.127732.
101. Zheng, S.; Jin, Z.; Han, C.; Li, J.; Xu, H.; Park, S.; Park, J.O.; Choi, E.; Xu, K. Graphene quantum dots-decorated hollow copper sulfide nanoparticles for controlled intracellular drug release and enhanced photothermal-chemotherapy. *J. Mater. Sci.* **2020**, *55*, 1184–1197, doi:10.1007/s10853-019-04062-x.
102. Thakur, M.; Kumawat, M.K.; Srivastava, R. Multifunctional graphene quantum dots for combined photothermal and photodynamic therapy coupled with cancer cell tracking applications. *RSC Adv.* **2017**, *7*, 5251–5261, doi:10.1039/c6ra25976f.
103. Liu, J.; Li, R.; Yang, B. Carbon Dots: A New Type of Carbon-Based Nanomaterial with Wide Applications. *ACS Cent. Sci.* **2020**, *6*, 2179–2195, doi:10.1021/acscentsci.0c01306.
104. Jiang, K.; Wang, Y.; Gao, X.; Cai, C.; Lin, H. Facile, Quick, and Gram-Scale Synthesis of Ultralong-Lifetime Room-Temperature-Phosphorescent Carbon Dots by Microwave Irradiation. *Angew. Chemie Int. Ed.* **2018**, *57*, 6216–6220, doi:https://doi.org/10.1002/anie.201802441.
105. Liu, M.L.; Chen, B. Bin; Li, C.M.; Huang, C.Z. Carbon dots: Synthesis, formation mechanism, fluorescence origin and sensing applications. *Green Chem.* **2019**, *21*, 449–471, doi:10.1039/c8gc02736f.
106. Zhang, Z.; Yi, G.; Li, P.; Zhang, X.; Fan, H.; Zhang, Y.; Wang, X.; Zhang, C. A minireview on doped carbon dots for photocatalytic and electrocatalytic applications. *Nanoscale* **2020**, *12*, 13899–13906, doi:10.1039/d0nr03163a.
107. Jia, Q.; Zhao, Z.; Liang, K.; Nan, F.; Li, Y.; Wang, J.; Ge, J.; Wang, P. Recent advances and prospects of carbon dots in cancer nanotheranostics. *Mater. Chem. Front.* **2020**, *4*, 449–471, doi:10.1039/c9qm00667b.
108. Boakye-Yiadom, K.O.; Kesse, S.; Opoku-Damoah, Y.; Filli, M.S.; Aquib, M.; Joelle, M.M.B.; Farooq, M.A.; Mavlyanova, R.; Raza, F.; Bavi, R.; et al. Carbon dots: Applications in bioimaging and theranostics. *Int. J. Pharm.* **2019**, *564*, 308–317, doi:10.1016/j.ijpharm.2019.04.055.
109. Li, Y.; Zheng, X.; Zhang, X.; Liu, S.; Pei, Q.; Zheng, M.; Xie, Z. Porphyrin-Based Carbon Dots for Photodynamic Therapy of Hepatoma. *Adv. Healthc. Mater.* **2017**, *6*, 1600924, doi:https://doi.org/10.1002/adhm.201600924.

110. Huang, P.; Lin, J.; Wang, X.; Wang, Z.; Zhang, C.; He, M.; Wang, K.; Chen, F.; Li, Z.; Shen, G.; et al. Light-Triggered Theranostics Based on Photosensitizer-Conjugated Carbon Dots for Simultaneous Enhanced-Fluorescence Imaging and Photodynamic Therapy. *Adv. Mater.* **2012**, *24*, 5104–5110, doi:https://doi.org/10.1002/adma.201200650.
111. Qin, X.; Liu, J.; Zhang, Q.; Chen, W.; Zhong, X.; He, J. Synthesis of Yellow-Fluorescent Carbon Nano-dots by Microplasma for Imaging and Photocatalytic Inactivation of Cancer Cells. *Nanoscale Res. Lett.* **2021**, *16*, doi:10.1186/s11671-021-03478-2.
112. Nocito, G.; Calabrese, G.; Forte, S.; Petralia, S.; Puglisi, C.; Campolo, M.; Esposito, E.; Conoci, S. Carbon dots as promising tools for cancer diagnosis and therapy. *Cancers (Basel).* **2021**, *13*, 1–14, doi:10.3390/cancers13091991.
113. Meena, R.; Singh, R.; Marappan, G.; Kushwaha, G.; Gupta, N.; Meena, R.; Gupta, J.P.; Agarwal, R.R.; Fahmi, N.; Kushwaha, O.S. Fluorescent carbon dots driven from ayurvedic medicinal plants for cancer cell imaging and phototherapy. *Heliyon* **2019**, *5*, e02483, doi:10.1016/j.heliyon.2019.e02483.
114. Sun, S.; Zhang, L.; Jiang, K.; Wu, A.; Lin, H. Toward High-Efficient Red Emissive Carbon Dots: Facile Preparation, Unique Properties, and Applications as Multifunctional Theranostic Agents. *Chem. Mater.* **2016**, *28*, 8659–8668, doi:10.1021/acs.chemmater.6b03695.
115. Geng, B.; Yang, D.; Pan, D.; Wang, L.; Zheng, F.; Shen, W.; Zhang, C.; Li, X. NIR-responsive carbon dots for efficient photothermal cancer therapy at low power densities. *Carbon N. Y.* **2018**, *134*, 153–162, doi:10.1016/j.carbon.2018.03.084.
116. Zhang, M.; Wang, W.; Cui, Y.; Chu, X.; Sun, B.; Zhou, N.; Shen, J. Magnetofluorescent Fe3O4/carbon quantum dots coated single-walled carbon nanotubes as dual-modal targeted imaging and chemo/photodynamic/photothermal triple-modal therapeutic agents. *Chem. Eng. J.* **2018**, *338*, 526–538, doi:10.1016/j.cej.2018.01.081.
117. Jia, Q.; Zheng, X.; Ge, J.; Liu, W.; Ren, H.; Chen, S.; Wen, Y.; Zhang, H.; Wu, J.; Wang, P. Synthesis of carbon dots from Hypocrella bambusae for bimodel fluorescence/photoacoustic imaging-guided synergistic photodynamic/photothermal therapy of cancer. *J. Colloid Interface Sci.* **2018**, *526*, 302–311, doi:10.1016/j.jcis.2018.05.005.
118. Zhao, S.; Wu, S.; Jia, Q.; Huang, L.; Lan, M.; Wang, P.; Zhang, W. Lysosome-targetable carbon dots for highly efficient photothermal/photodynamic synergistic cancer therapy and photoacoustic/two-photon excited fluorescence imaging. *Chem. Eng. J.* **2020**, *388*, 124212, doi:10.1016/j.cej.2020.124212.
119. Lan, M.; Guo, L.; Zhao, S.; Zhang, Z.; Jia, Q.; Yan, L.; Xia, J.; Zhang, H.; Wang, P.; Zhang, W. Carbon Dots as Multifunctional Phototheranostic Agents for Photoacoustic/Fluorescence Imaging and Photothermal/Photodynamic Synergistic Cancer Therapy. *Adv. Ther.* **2018**, *1*, 1800077, doi:10.1002/adtp.201800077.
120. Sun, S.; Chen, J.; Jiang, K.; Tang, Z.; Wang, Y.; Li, Z.; Liu, C.; Wu, A.; Lin, H. Ce6-Modified Carbon Dots for Multimodal-Imaging-Guided and Single-NIR-Laser-Triggered Photothermal/Photodynamic Synergistic Cancer Therapy by Reduced Irradiation Power. *ACS Appl. Mater. Interfaces* **2019**, *11*, 5791–5803, doi:10.1021/acsami.8b19042.
121. Guo, X.L.; Ding, Z.Y.; Deng, S.M.; Wen, C.C.; Shen, X.C.; Jiang, B.P.; Liang, H. A novel strategy of transition-metal doping to engineer absorption of carbon dots for near-infrared photothermal/photodynamic therapies. *Carbon N. Y.* **2018**, *134*, 519–530, doi:10.1016/j.carbon.2018.04.001.
122. Yang, W.; Wei, B.; Yang, Z.; Sheng, L. Facile synthesis of novel carbon-dots/hemin nanoplatforms for synergistic photo-thermal and photo-dynamic therapies. *J. Inorg. Biochem.* **2019**, *193*, 166–172, doi:10.1016/j.jinorgbio.2019.01.018.
123. Zhao, S.; Wu, S.; Jia, Q.; Huang, L.; Lan, M.; Wang, P.; Zhang, W. Lysosome-targetable carbon dots for highly efficient photothermal/photodynamic synergistic cancer therapy and photoacoustic/two-photon excited fluorescence imaging. *Chem. Eng. J.* **2020**, *388*, 124212, doi:10.1016/j.cej.2020.124212.
124. Madannejad, R.; Shoaie, N.; Jahanpeyma, F.; Darvishi, M.H.; Azimzadeh, M.; Javadi, H. Toxicity of carbon-based nanomaterials: Reviewing recent reports in medical and biological systems. *Chem. Biol. Interact.* **2019**, *307*, 206–222, doi:10.1016/j.cbi.2019.04.036.
125. Fard, J.K.; Jafari, S.; Eghbal, M.A. A Review of Molecular Mechanisms Involved in Toxicity of Nanoparticles. *Tabriz Univ. Med. Sci.* **2015**, *5*, 447–454, doi:10.15171/apb.2015.061.
126. Pelin, M.; Fusco, L.; Martín, C.; Sosa, S.; Frontiñán-Rubio, J.; González-Domínguez, J.M.; Durán-Prado, M.; Vázquez, E.; Prato, M.; Tubaro, A. Graphene and graphene oxide induce ROS production in human HaCaT skin keratinocytes: The role of xanthine oxidase and NADH dehydrogenase. *Nanoscale* **2018**, *10*, 11820–11830, doi:10.1039/c8nr02933d.
127. Koike, E.; Kobayashi, T. Chemical and biological oxidative effects of carbon black nanoparticles. *Chemosphere* **2006**, *65*, 946–951, doi:10.1016/j.chemosphere.2006.03.078.
128. Liao, C.; Li, Y.; Tjong, S.C. Graphene nanomaterials: Synthesis, biocompatibility, and cytotoxicity. *Int. J. Mol. Sci.* **2018**, *19*, doi:10.3390/ijms19113564.
129. Chuang, H.C.; Chen, L.C.; Lei, Y.C.; Wu, K.Y.; Feng, P.H.; Cheng, T.J. Surface area as a dose metric for carbon black nanoparticles: A study of oxidative stress, DNA single-strand breakage and inflammation in rats. *Atmos. Environ.* **2015**, *106*, 329–334, doi:10.1016/j.atmosenv.2015.02.014.
130. Zhang, Y.; Petibone, D.; Xu, Y.; Mahmood, M.; Karmakar, A.; Casciano, D.; Ali, S.; Biris, A.S. Toxicity and efficacy of carbon nanotubes and graphene: The utility of carbon-based nanoparticles in nanomedicine. *Drug Metab. Rev.* **2014**, *46*, 232–246, doi:10.3109/03602532.2014.883406.
131. Liu, C.W.; Xiong, F.; Jia, H.Z.; Wang, X.L.; Cheng, H.; Sun, Y.H.; Zhang, X.Z.; Zhuo, R.X.; Feng, J. Graphene-based anticancer nanosystem and its biosafety evaluation using a zebrafish model. *Biomacromolecules* **2013**, *14*, 358–366, doi:10.1021/bm3015297.

132. Seabra, A.B.; Paula, A.J.; De Lima, R.; Alves, O.L.; Durán, N. Nanotoxicity of graphene and graphene oxide. *Chem. Res. Toxicol.* **2014**, *27*, 159–168, doi:10.1021/tx400385x.
133. Alternative, T.-P.S.; Oxide, G.; Applications, B. Amine-Modi fi ed Graphene : Thrombo- Protective Safer Alternative to Graphene Oxide for Biomedical. **2012**, 2731–2740.
134. Yuan, X.; Zhang, X.; Sun, L.; Wei, Y.; Wei, X. Cellular Toxicity and Immunological Effects of Carbon-based Nanomaterials. *Part. Fibre Toxicol.* **2019**, *16*, doi:10.1186/s12989-019-0299-z.
135. Lindberg, H.K.; Falck, G.C.M.; Suhonen, S.; Vippola, M.; Vanhala, E.; Catalán, J.; Savolainen, K.; Norppa, H. Genotoxicity of nanomaterials: DNA damage and micronuclei induced by carbon nanotubes and graphite nanofibres in human bronchial epithelial cells in vitro. *Toxicol. Lett.* **2009**, *186*, 166–173, doi:10.1016/j.toxlet.2008.11.019.
136. Hurt, R.H.; Monthioux, M.; Kane, A. Toxicology of carbon nanomaterials: Status, trends, and perspectives on the special issue. *Carbon N. Y.* **2006**, *44*, 1028–1033, doi:10.1016/j.carbon.2005.12.023.
137. Yang, K.; Gong, H.; Shi, X.; Wan, J.; Zhang, Y.; Liu, Z. In vivo biodistribution and toxicology of functionalized nano-graphene oxide in mice after oral and intraperitoneal administration. *Biomaterials* **2013**, *34*, 2787–2795, doi:10.1016/j.biomaterials.2013.01.001.
138. Yan, L.; Wang, Y.; Xu, X.; Zeng, C.; Hou, J.; Lin, M.; Xu, J.; Sun, F.; Huang, X.; Dai, L.; et al. Can graphene oxide cause damage to eyesight? *Chem. Res. Toxicol.* **2012**, *25*, 1265–1270, doi:10.1021/tx300129f.
139. Heister, E.; Brunner, E.W.; Dieckmann, G.R.; Jurewicz, I.; Dalton, A.B. Are carbon nanotubes a natural solution? applications in biology and medicine. *ACS Appl. Mater. Interfaces* **2013**, *5*, 1870–1891, doi:10.1021/am302902d.